AJNR

Analysis of Flow Dynamics and Outcomes of Cerebral Aneurysms Treated with Intrasaccular Flow-Diverting Devices

J.R. Cebral, B.J. Chung, F. Mut, J. Chudyk, C. Bleise, E. Scrivano, P. Lylyk, R. Kadirvel and D. Kallmes

AJNR Am J Neuroradiol 2019, 40 (9) 1511-1516
doi: https://doi.org/10.3174/ajnr.A6169
http://www.ajnr.org/content/40/9/1511

Analysis of Flow Dynamics and Outcomes of Cerebral Aneurysms Treated with Intrasaccular Flow-Diverting Devices

J.R. Cebral, B.J. Chung, F. Mut, J. Chudyk, C. Bleise, E. Scrivano, P. Lylyk, R. Kadirvel, and D. Kallmes

ABSTRACT

BACKGROUND AND PURPOSE: Intrasaccular flow diversion offers a promising treatment option for complex bifurcation aneurysms. The purpose of this study was to compare the flow conditions between successfully occluded and incompletely occluded aneurysms treated with intrasaccular devices.

MATERIALS AND METHODS: The hemodynamics in 18 completely occluded aneurysms after treatment with intrasaccular devices was compared against 18 that were incompletely occluded at follow-up. Hemodynamic and geometric parameters were obtained from computational fluid dynamics models constructed from 3D angiographies. Models of the intrasaccular devices were created and interactively deployed within the vascular models using posttreatment angiography images for guidance. Hemodynamic and geometric variables were compared using the Mann-Whitney test and univariate logistic regression analysis.

RESULTS: Incomplete occlusion was associated with large posttreatment mean aneurysm inflows ($P = .02$) and small reductions in the mean inflow rate ($P = .01$) and inflow concentration index ($P = .03$). Incompletely occluded aneurysms were larger ($P = .002$) and had wider necks ($P = .004$) than completely occluded aneurysms and tended to have more complex flow patterns, though this trend was not significant after adjusting for multiple testing.

CONCLUSIONS: The outcome of cerebral aneurysm treatment with intrasaccular flow diverters is associated with flow conditions created immediately after device implantation. Flow conditions unfavorable for immediate and complete occlusion seem to be created by improper positioning or orientation of the device. Complete occlusion is more difficult to achieve in larger aneurysms, aneurysms with wider necks, and aneurysms with stronger and more complex flows.

ABBREVIATIONS: AR = aspect ratio; Asize = aneurysm size; AUC = area under the curve; BF = bottleneck factor; corelen = vortex corelen length; ICI = inflow concentration index; UI = undulation index; NSI = nonsphericity index; Nsize = neck size; Q = mean aneurysm inflow; Qpost = posttreatment aneurysm inflow rate; VE = mean aneurysm velocity; VO = mean vorticity; VOR = volume-to-ostium ratio

Flow diversion (ie, the endoluminal placement of a flow-diverting stent) has become an attractive treatment option for many large and complex aneurysms in which coiling alone tends to have high rates of recompaction and recanalization.[1] However, these flow-diversion techniques are not free of complications. Problems associated with the treatment of cerebral aneurysms with endoluminal flow diverters include incomplete occlusion or persistent filling of the aneurysm, thromboembolic events, in-stent stenosis or myointimal hyperplasia, delayed aneurysm rupture, and delayed distal hemorrhage.[2,3] In addition, 2 further concerns are the use of dual-antiplatelet therapy, which increases the chances of other complications, and the treatment of bifurcation aneurysms in which at least 1 of the daughter branches would be jailed by endoluminal devices, which increases the chances of thromboembolic events or vessel occlusions.

Intrasaccular flow-diverting devices offer the possibility of addressing some of these concerns.[4-6] The devices have been developed specifically for bifurcation aneurysms, and most cases do not require the use of dual-antiplatelet therapy as with endoluminal devices. Therefore, they constitute a promising approach for

Received February 27, 2019; accepted after revision July 3.

From the Bioengineering Department (J.R.C., F.M.), Volgenau School of Engineering, George Mason University, Fairfax, Virginia; Department of Mathematical Sciences (B.J.C.), Montclair State University, Montclair, New Jersey; Department of Interventional Neuroradiology (J.C., C.B., E.S., P.L.), Clinica ENERI, Buenos Aires, Argentina; and Department of Interventional Neuroradiology (R.K., D.K.), Mayo Clinic, Rochester, Minnesota.

This work was supported by the National Institutes of Health, grant No. R01 NS076491.

Please address correspondence to Juan R. Cebral, PhD, Bioengineering and Mechanical Engineering Departments, Volgenau School of Engineering, George Mason University, 4400 University Dr, MSN 1J7, Fairfax, VA 22030; e-mail: jcebral@gmu.edu

http://dx.doi.org/10.3174/ajnr.A6169

complex bifurcation aneurysms[7] and an alternative to other techniques such as Y-stent placement and coiling.[8,9] However, not all aneurysms are immediately occluded after implantation of intrasaccular flow diverters. Thus, the objective of our study was to identify aneurysm and flow characteristics (and their change) associated with subsequent outcome after intrasaccular device implantation (ie, complete or incomplete occlusion). This information is important to understand the reasons underlying failures, pinpoint problematic cases, and enable the prediction of long-term outcomes to improve treatment planning and device selection.

MATERIALS AND METHODS

Data

A total of 42 aneurysms in 39 patients (35 women and 4 men; mean age, 64 years) treated with intrasaccular devices were studied. The aneurysms were imaged with 3D rotational angiography immediately before treatment. 2D-DSA images were acquired immediately before and after implantation of the intrasaccular devices. All aneurysms were treated with the Woven EndoBridge (WEB; Sequent Medical, Aliso Viejo, California) device,[4] 33 with Dual-Layer (DL), 8 with Single-Layer (SL), and 1 with a Single-Layer Spherical (SLS) devices. Typically, the device size is chosen to be 1 mm larger in diameter compared with the aneurysm width and 1 mm smaller in length than the aneurysm depth (size from the neck to the dome), to allow the device to expand into the aneurysm dome and conform to the aneurysm walls. Of the 42 aneurysms, 6 were discarded because there were no follow-up angiographic studies to evaluate the treatment outcome. Patient, aneurysm, and device characteristics of the remaining 36 aneurysms in 33 patients are summarized in On-line Table 1.

Models

Patient-specific vascular models were constructed from the 3D rotational angiography images using previously developed methods.[10] Unstructured grids composed of tetrahedral elements that fill the lumen of the vascular models were constructed using an advancing front grid generator.[10] Models of the intrasaccular devices were created and interactively placed within the vascular models using DSA image-guidance tools and techniques recently developed.[11] Briefly, the vascular model is rendered semitransparent and is superimposed on the DSA image; it is then interactively rotated, zoomed, and translated to make sure it coincides with the vessels visible in the DSA image (ie, both have the same projection). Next, the device is interactively translated and rotated to make the virtual device markers coincide with the actual device markers visible in the DSA image. The process is repeated with different DSA images acquired in different projections (ie, different views) to guide the placement of the 3D virtual device within the vascular model. The process is illustrated with a representative case in On-line Fig 1.

Computational fluid dynamics simulations were performed by numerically solving the Navier-Stokes equations using an in-house finite-element solver.[12] Pulsatile flow conditions were imposed at the inlet boundary by scaling flow waveforms measured in healthy subjects.[13] To simulate the blood flow after intrasaccular device implantation, we used an immersed boundary method operating on adaptive unstructured grids.[14] In this approach, the device wires were discretized as a series of overlapping spheres and the mesh elements intersected by the spheres were adaptively refined to resolve the wires. Single-layer devices were modeled as a structure composed of 144 wires of 25 μm in diameter braided at an angle of 80°. Double-layer devices of >8 mm were modeled as an outer layer of 144 wires of 19 μm in diameter and an inner layer of 144 wires of 38 μm in diameter, both braided at an angle of 80°. Double-layer devices <8 mm had 108 wires in each layer instead of 144. Because these devices contain numerous thin wires, the resulting meshes after adaptive refinement were quite large, ranging between 100 and 200 million tetrahedra.

Flow simulations were performed for 2 cardiac cycles, and the results from the second cycle were used to compute a number of flow parameters to quantitatively characterize the aneurysm hemodynamic environment.[15] In particular, these variables characterize the mean aneurysm inflow (Q) and concentration (ICI) of the inflow jet, and the mean aneurysm velocity (VE) and mean vorticity (VO, corelen) of the intra-aneurysmal flow pattern. Similarly, a number of geometric parameters were calculated to characterize the size (aneurysm size [Asize], neck size [Nsize]) and shape (aspect ratio [AR], bottleneck factor [BF], volume-to-ostium ratio [VOR], undulation index [UI], nonsphericity index [NSI]) of the aneurysms.[16] A list of the geometric and hemodynamic variables used and their basic meaning are provided in On-line Table 2. Hemodynamic analysis was performed blinded to aneurysm occlusion outcomes.

Analysis

The outcomes of the treatments were evaluated at follow-up with angiography imaging. Aneurysms were classified into 4 categories: A) no remnant or filling of the aneurysm or device, B) small remnant associated with filling of the proximal recession of the device, C) filling of the proximal compartment of the device (dual-layer only), and D) filling of the distal compartment of the device. Categories A and B were grouped into a "complete" occlusion group, and categories C and D, into an "incomplete" occlusion group. Outcome assessment was performed blinded to the computational fluid dynamics results.

Hemodynamic variables computed for the pretreatment and posttreatment configurations, as well as their percentage change (reduction) from pre- to posttreatment, were compared between the complete and incomplete occlusion groups using the nonparametric Mann-Whitney test. Geometric characteristics of the aneurysms of these 2 groups were similarly compared. Differences were considered significant at $P < .05$ (95% confidence). P values were adjusted for multiple comparisons using the Bonferroni method. For each of the variables with statistically significant differences, univariate logistic regressions were performed, receiver operating characteristic curves were created, and the area under the curve (AUC) was calculated to assess the discriminatory power of each of these variables. Optimal thresholds were computed as the point on the receiver operating characteristic curve closest to the upper-left corner. Multivariate logistic regression analysis was performed with statistically significant variables. All statistical analyses were performed using codes written in R statistical and computing software (http://www.r-project.org/).

Table 1: Hemodynamic parameters before treatment, after treatment, and their change (reduction), along with geometric characteristics of aneurysms in the complete and incomplete occlusion groups[a]

Variable	Complete (*n* = 18)		Incomplete (*n* = 18)		Comparison			
	Mean	SD	Mean	SD	*P*	*P* Adjusted	AUC	Threshold
Geometry								
Asize	0.781	0.131	1.060	0.213	<.001[b]	.002[b]	0.87	1.04
Nsize	0.502	0.097	0.660	0.132	<.001[b]	.004[b]	0.85	0.70
AR	1.335	0.424	1.507	0.352	.11	.85		
BF	1.349	0.215	1.483	0.190	.05	.53		
VOR	0.776	0.390	1.258	0.500	.004[b]	.06	0.79	1.15
UI	0.124	0.046	0.097	0.052	.09	.77		
NSI	0.190	0.042	0.192	0.030	.71	1.00		
Pre-Tx hemodynamics								
ICI	1.57	0.85	1.72	0.59	.29	1.00		
Q	1.09	0.59	1.67	0.78	.02[b]	.26	0.74	1.60
VE	14.75	8.87	13.79	7.08	.81	1.00		
VO	405.54	272.72	317.64	196.43	.54	1.00		
Corelen	1.99	0.95	4.47	3.60	.04[b]	.49	0.71	6.54
Post-Tx hemodynamics								
ICI	1.03	1.13	1.65	1.01	.03[b]	.37	0.72	2.05
Q	0.61	0.50	1.49	0.96	.001[b]	.02[b]	0.82	1.64
VE	3.15	2.90	4.72	4.44	.18	1.00		
VO	130.07	107.78	148.18	128.19	.54	1.00		
Corelen	37.95	41.87	55.34	28.82	.02[b]	.35	0.73	84.32
Hemodynamic reduction (%)								
ΔICI	46.39	34.55	8.07	32.45	.002[b]	.03[b]	0.81	29.17
ΔQ	47.46	28.25	9.93	33.41	<.001[b]	.01[b]	0.83	30.10
ΔVE	80.88	11.19	62.90	36.63	.03[b]	.41	0.72	20.41
ΔVO	67.40	13.96	46.11	44.86	.04[b]	.49	0.70	−8.83
Δcorelen	−1855.60	1721.87	−2068.93	1965.52	.81	1.00		

Note:—Pre-Tx indicates pretreatment; Post-Tx, posttreatment.

[a] Results of univariate analysis between these 2 aneurysm groups.

[b] Statistically significant differences ($P < .05$).

RESULTS

Of the 36 aneurysms with follow-up included in the study, 18 were classified into the complete occlusion group and 18 into the incomplete occlusion group. The mean and SD of geometric and hemodynamic variables (and their percentage change) in each aneurysm group are presented in Table 1. The *P* values of the Mann-Whitney univariate tests and the *P* values adjusted for multiple testing are provided, and significant differences are indicated by footnote b. The AUC and optimal threshold for the univariate logistic regressions are provided for variables with statistically significant differences between complete and incomplete occlusion groups.

These results indicate that large posttreatment aneurysm inflow rates (Q, $P = .02$) and small reductions in inflow (ΔQ, $P = .01$) and inflow concentration (ΔICI, $P = .03$) from pre- to posttreatment are associated with incomplete occlusion. Pre- and posttreatment flows tended to be more complex (ie, larger vortex corelen length [corelen]) in incompletely occluded aneurysms compared with completely occluded aneurysms, but these differences were not significant when adjusting for multiple testing.

Geometrically, incompletely occluded aneurysms were larger (Asize, $P = .002$) with wider necks (Nsize, $P = .004$) than completely occluded aneurysms. Incompletely occluded aneurysms also tended to have larger volume-to-ostium ratios (ie, larger cavities for similar neck sizes), but this association only reached marginal statistical significance after adjusting for multiple testing (VOR, $P = .06$).

Multivariate statistical logistic regression was performed with the statistically significant variables (Asize, Nsize, posttreatment aneurysm inflow rate [Qpost], ΔQ, and ΔICI). Stepwise variable selection using the Akaike information criterion retained Asize, Nsize, and Qpost as independent predictors of incomplete occlusion with an AUC = 0.93 and a prediction error of 22% during cross-validation (On-line Fig 2). The linearized model coefficients (measure of the relative importance of the variables) were Asize = 4.58, Nsize = 2.35, Qpost = 3.87.

DISCUSSION

Associations with Incomplete Occlusion

The results of this study indicate that incomplete aneurysm occlusion after treatment with intrasaccular flow diverters is associated with a high persistent inflow rate into the aneurysm immediately after treatment and a small reduction in the inflow rate (and inflow jet concentration) from pre- to posttreatment conditions. These results are not surprising and are consistent with previous studies analyzing the relationship between flow conditions and outcomes of aneurysms treated with endoluminal flow diverters.[17-19] Furthermore, our results suggest that the change in inflow rate (ΔQ) from pre- to posttreatment, and/or the final posttreatment inflow rate could discriminate between incomplete and complete occlusions at follow-up with a predictive power of approximately 82%–83%, as suggested by the corresponding AUCs. Our results also indicate that, in general, it is more difficult to achieve complete occlusions in larger aneurysms, aneurysms with wider necks, and aneurysms with stronger and more complex flows. The multivariate analysis suggests that adding flow information (especially posttreatment inflow rate) improves the

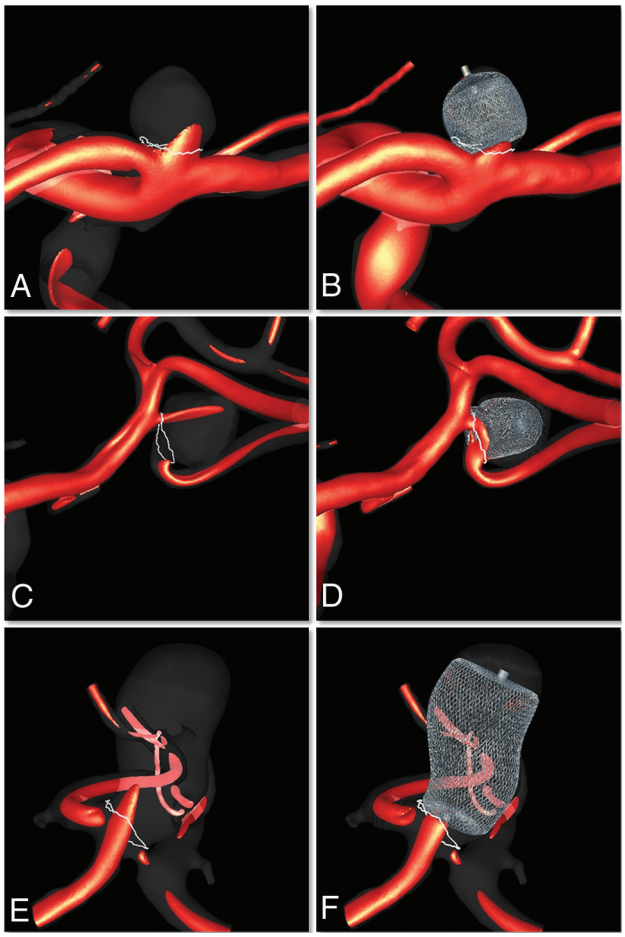

FIG 1. Examples of 3 aneurysms treated with intrasaccular devices that are completely occluded at follow-up. Left column (*A*, *C*, and *E*) shows visualizations of the inflow jet before treatment, and right column (*B*, *D*, and *F*) shows corresponding visualizations immediately after treatment. *Upper row*, ICA bifurcation aneurysm. *Center row*, MCA bifurcation aneurysm. *Lower row*, Anterior communicating artery aneurysm.

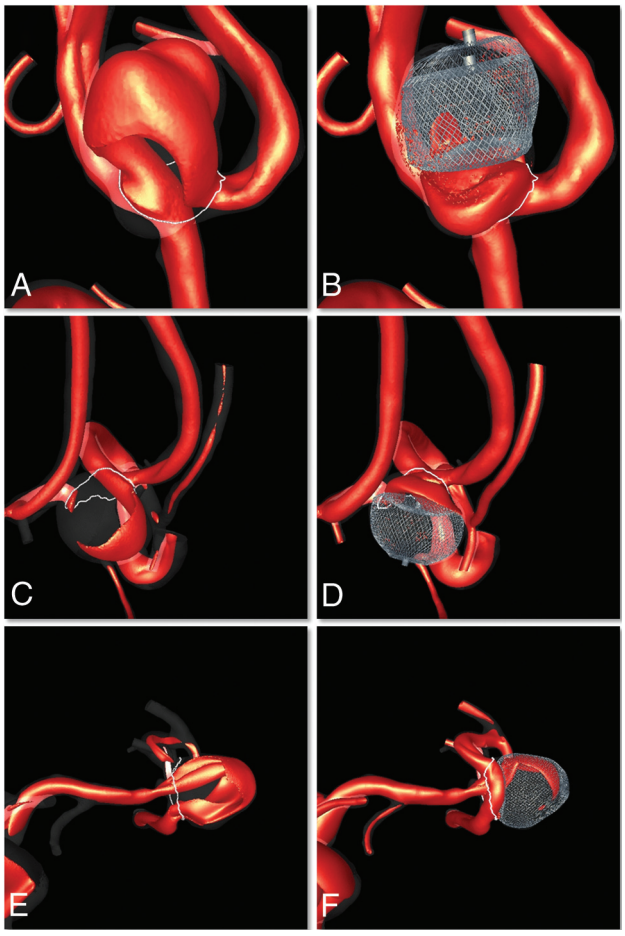

FIG 2. Examples of 3 aneurysms treated with intrasaccular devices that are incompletely occluded at follow-up. Left column (*A*, *C*, and *E*) shows visualizations of the inflow jet before treatment, and right column (*B*, *D*, and *F*) shows corresponding visualizations immediately after treatment. All 3 aneurysms were at the MCA bifurcation.

assessment of future occlusion based on geometry alone. Furthermore, according to the linearized coefficients of this model, aneurysm size and inflow rate seem to be the most important variables to predict or explain outcomes.

Previous studies have proposed the mean aneurysm flow amplitude ratio, derived from dynamic DSA images, as a predictor of aneurysm occlusion after flow diversion.[20] Additionally, a previous study showed that mean aneurysm flow amplitude is related to the VE determined through computational fluid dynamics analysis.[21] Most interesting, in our study, the reduction in the mean aneurysm flow velocity (ΔVE) tended to be larger in completely occluded aneurysms compared with incompletely occluded aneurysms, but this trend did not achieve statistical significance when adjusting for multiple comparisons. Nevertheless, our univariate logistic regression analysis indicated that ΔVE (and thus perhaps the mean aneurysm flow amplitude ratio) could discriminate between complete and incomplete occlusions with approximately 72% accuracy (AUC = 0.72).

Examples of 3 aneurysms in the complete occlusion group are shown in Fig 1. This figure presents visualizations of the inflow jet before and after treatment. A noticeable reduction in the inflow jet into the aneurysm can be observed in these 3 cases. Similarly, examples of 3 aneurysms in the incomplete occlusion group are presented in Fig 2. In the first case (upper row), it can be seen that the position of the device is not optimal—that is, the device is not well-apposed to the walls at the aneurysm opening but further into the sac, allowing flow into the aneurysm. In the second case (center row), there seems to be substantial flow into the aneurysm because of suboptimal orientation of the base of the device with respect to the aneurysm opening. In the third case (lower row), though the device seems properly placed, the inflow jet is quite strong and is not sufficiently disrupted by the device. These results seem to be consistent with a previous study of endoluminal flow diversion that indicated that proper sizing of the stent (which produces minimal change in the device cells compared with its reference configuration) is associated with a higher rate of complete aneurysm occlusion.[22]

Clinical Implications

Our findings indicate that treatment failure (ie, incomplete occlusion) could result not only because of poor device deployment (which is more common in large aneurysms with wide necks) but also because the devices may not provide sufficient flow disruption, even if appropriately placed, in cases with strong inflow jets.

Therefore, in addition to the aneurysm geometric features that predispose them to failure (size and neck), knowledge of pretreatment flow characteristics (in particular the location and strength of the inflow jet) could help select devices (porosity) and place them optimally to achieve the largest flow disruption possible (lower porosity regions blocking the inflow jet). Additional quantitative knowledge of posttreatment flow conditions could also be used to predict outcomes using statistical models such as the multivariate logistic model presented here. This information is valuable for evaluating the procedure and potentially recommending further steps (eg, deployment of a flow-diverting stent if failure is anticipated). This hemodynamic information could potentially be derived from computational fluid dynamics models, but this step would require significantly reducing the time required for posttreatment computational fluid dynamics simulations. This could be achieved with steady-state simulations (and perhaps reduced vascular models) that can yield mean flow quantities such as the ones presented here in a much shorter time (minutes). Alternatively, flow conditions could be potentially inferred from in vivo measurements such as the mean aneurysm flow amplitude derived from dynamic DSA images (though these techniques would have to be improved for estimating flows in the presence of intrasaccular devices).

Limitations

Patient-specific flow conditions were unavailable; therefore, they were adapted from measurements in healthy subjects. Vessel walls were approximated as rigid, and blood, as a continuous Newtonian fluid. There are uncertainties associated with the exact placement of the virtual devices inside the vascular model. Our interactive image-guided device-placement approach attempted to minimize these uncertainties by reproducing the position and orientation of the device by visually matching the virtual and actual device markers visible in the DSA images from all available viewpoints. Finally, our findings should be further confirmed with larger samples and more aneurysms at different locations.

CONCLUSIONS

The outcomes of cerebral aneurysm treatment with intrasaccular flow-diverting devices are associated with the flow conditions created immediately after implantation of these devices. In particular, a high posttreatment aneurysm inflow rate and a small reduction in the inflow rate (and inflow jet concentration) from pre- to posttreatment conditions are associated with incomplete occlusions. Flow conditions unfavorable for immediate and complete occlusions can be created by improper positioning or orientation of the device. Complete occlusions are more difficult to achieve in larger aneurysms, aneurysms with wider necks, and aneurysms with stronger and more complex flows.

Disclosures: Juan R. Cebral—*RELATED*: *Grant*: National Institutes of Health, *Comments*: research grant*; *UNRELATED: Grants/Grants Pending*: National Institutes of Health/Philips Healthcare, *Comments*: research grants.* Fernando Mut—*RELATED*: *Grant*: National Institutes of Health.* David Kallmes—*RELATED*: *Grant*: MicroVention/Sequent Medical, *Comments*: grant for preclinical research*; *UNRELATED*: *Grants/Grants Pending*: Medtronic, NeuroSigma, Neurogami Medical, *Comments*: support for preclinical research*; *Stock/Stock Options*: Superior Medical Experts, *Comments*: Founder. *Money paid to the institution.

REFERENCES

1. Pierot L, Biondi A. **Endovascular techniques for the management of wide-neck intracranial bifurcation aneurysms: a critical review of the literature.** *J Neuroradiol* 2016;43:167–75 CrossRef Medline
2. Zhou G, Su M, Yin YL, et al. **Complications associated with the use of flow-diverting devices for cerebral aneurysms: a systematic review and meta-analysis.** *Neurosurg Focus* 2017;42:E17 CrossRef Medline
3. Simgen A, Ley D, Roth C, et al. **Evaluation of occurring complications after flow diverter treatment of elastase-induced aneurysm in rabbits using micro-CT and MRI at 9.4 T.** *Neuroradiology* 2016;58:987–96 CrossRef Medline
4. Ding YH, Lewis DA, Kadirvel R, et al. **The Woven EndoBridge: a new aneurysm occlusion device.** *AJNR Am J Neuroradiol* 2011;32:607–11 CrossRef Medline
5. Pierot L, Liebig T, Sychra V, et al. **Intrasaccular flow-disruption treatment of intracranial aneurysms: preliminary results of a multicenter clinical study.** *AJNR Am J Neuroradiol* 2012;33:1232–38 CrossRef Medline
6. Lubicz B, Mine B, Collignon L, et al. **WEB device for endovascular treatment of wide-neck bifurcation aneurysms.** *AJNR Am J Neuroradiol* 2013;34:1209–14 CrossRef Medline
7. Pierot L, Klisch J, Cognard C, et al. **Endovascular WEB flow disruption in middle cerebral artery aneurysms: preliminary feasibility, clinical, and anatomical results in a multicenter study.** *Neurosurgery* 2013;73:27–34; discussion 34–35 CrossRef Medline
8. Yavuz K, Geyik S, Cekirge S, et al. **Double stent-assisted coil embolization treatment for bifurcation aneurysms: immediate treatment results and long-term angiographic outcome.** *AJNR Am J Neuroradiol* 2013;34:1778–84 CrossRef Medline
9. Cekirge HS, Yavuz K, Geyik S, et al. **A novel "Y" stent flow diversion technique for the endovascular treatment of bifurcation aneurysms without endosaccular coiling.** *AJNR Am J Neuroradiol* 2011;32:1262–68 CrossRef Medline
10. Cebral JR, Castro MA, Appanaboyina S, et al. **Efficient pipeline for image-based patient-specific analysis of cerebral aneurysm hemodynamics: technique and sensitivity.** *IEEE Trans Med Imaging* 2005;24:457–67 CrossRef Medline
11. Mut F, Chung BJ, Chudyk J, et al. **Image-based modeling of blood flow in cerebral aneurysms treated with intrasaccular flow diverting devices.** *Int J Numer Method Biomed Eng* 2019;35:e3202 CrossRef Medline
12. Mut F, Aubry R, Löhner R, et al. **Fast numerical solutions of patient-specific blood flows in 3D arterial systems.** *Int J Numer Method Biomed Eng* 2010;26:73–85 CrossRef Medline
13. Cebral JR, Castro MA, Putman CM, et al. **Flow-area relationship in internal carotid and vertebral arteries.** *Physiol Meas* 2008;29:585–94 CrossRef Medline
14. Appanaboyina S, Mut F, Löhner R, et al. **Computational fluid dynamics of stented intracranial aneurysms using adaptive embedded unstructured grids.** *International Journal for Numerical Methods in Fluids* 2008;57:457–93 CrossRef
15. Mut F, Löhner R, Chien A, et al. **Computational hemodynamics framework for the analysis of cerebral aneurysms.** *Int J Numer Method Biomed Eng* 2011;27:822–39 CrossRef Medline
16. Raghavan ML, Ma B, Harbaugh RE. **Quantified aneurysm shape and rupture risk.** *J Neurosurg* 2005;102:355–62 CrossRef Medline
17. Kulcsár Z, Augsburger L, Reymond P, et al. **Flow diversion treatment: intra-aneurismal blood flow velocity and WSS reduction are parameters to predict aneurysm thrombosis.** *Acta Neurochir (Wien)* 2012;154:1827–34 CrossRef Medline
18. Cebral JR, Mut F, Raschi M, et al. **Analysis of hemodynamics and aneurysm occlusion after flow-diverting treatment in rabbit models.** *AJNR Am J Neuroradiol* 2014;35:1567–73 CrossRef Medline
19. Paliwal N, Damiano RJ, Davies JM, et al. **Association between hemodynamic modifications and clinical outcome of intracranial aneurysms treated using flow diverters.** *Proc SPIE Int Soc Opt Eng* 2017;10135 CrossRef Medline

20. Pereira VM, Bonnefous O, Ouared R, et al. **A DSA-based method using contrast-motion estimation for the assessment of the intra-aneurysmal flow changes induced by flow-diverter stents.** *AJNR Am J Neuroradiol* 2013;34:805–15 CrossRef Medline
21. Cebral JR, Mut F, Chung BJ, et al. **Understanding angiography-based aneurysm flow fields through comparison with computational fluid dynamics.** *AJNR Am J Neuroradiol* 2017;38:1180–86 CrossRef Medline
22. Herbreteau D, Bibi R, Narata AP, et al. **Are anatomic results influenced by WEB shape modification? Analysis in a prospective, single-center series of 39 patients with aneurysms treated with the WEB.** *AJNR Am J Neuroradiol* 2016;37:2280–86 CrossRef Medline